

Published in final edited form as:

Oncogene. 2017 April 20; 36(16): 2286–2296. doi:10.1038/onc.2016.382.

Genomic modelling of the ESR1 Y537S mutation for evaluating function and new therapeutic approaches for metastatic breast cancer

Alison Harrod¹, Joel Fulton¹, Van T.M. Nguyen¹, Manikandan Periyasamy¹, Laura Ramos Garcia¹, Chun-Fui Lai¹, Gergana Metodieva², Alexander de Giorgio¹, Rosa L. Williams¹, Daniela B. Santos¹, Paula Jimenez Gomez¹, Meng-Lay Lin¹, Metodi V. Metodiev², Justin Stebbing¹, Leandro Castellano¹, Luca Magnani¹, R. Charles Coombes¹, Laki Buluwela^{1,*}, and Simak Ali^{1,*}

¹Department of Surgery & Cancer, Imperial College London, Hammersmith Hospital Campus, London, UK

²School of Biological Sciences, University of Essex, Wivenhoe Park, Colchester, CO4 3SQ, UK

Abstract

Drugs that inhibit estrogen receptor- α (ER) activity have been highly successful in treating and reducing breast cancer progression in ER-positive disease. However, resistance to these therapies presents a major clinical problem. Recent genetic studies have shown that mutations in the ER gene are found in >20% of tumours that progress on endocrine therapies. Remarkably, the great majority of these mutations localise to just a few amino acids within or near the critical helix 12 region of the ER hormone binding domain, where they are likely to be single allele mutations. Understanding how these mutations impact on ER function is a prerequisite for identifying methods to treat breast cancer patients featuring such mutations. Towards this end, we used CRISPR-Cas9 genome editing to make a single allele knockin of the most commonly mutated amino acid residue, tyrosine 537, in the estrogen-responsive MCF7 breast cancer cell line. Genomic analyses using RNA-seq and ER ChIP-seq demonstrated that the Y537S mutation promotes constitutive ER activity globally, resulting in estrogen-independent growth. MCF7-Y537S cells were resistant to the anti-estrogen tamoxifen and fulvestrant. Further, we show that the basal transcription factor TFIID is constitutively recruited by ER-Y537S, resulting in ligand-independent phosphorylation of Serine 118 (Ser118) by the TFIID kinase, CDK7. The CDK7 inhibitor, THZ1 prevented Ser118 phosphorylation and inhibited growth of MCF7-Y537S cells. These studies confirm the functional importance of ER mutations in endocrine resistance, demonstrate the utility of knockin mutational models for investigating alternative therapeutic approaches and highlight CDK7 inhibition as a potential therapy for endocrine resistant breast cancer mediated by ER mutations.

Users may view, print, copy, and download text and data-mine the content in such documents, for the purposes of academic research, subject always to the full Conditions of use:http://www.nature.com/authors/editorial_policies/license.html#terms

*Authors for correspondence: Laki Buluwela or Simak Ali, Department of Surgery & Cancer, Imperial College London, Du Cane Road, London W12 0NN, UK l.buluwela@imperial.ac.uk; simak.ali@imperial.ac.uk.

Keywords

breast cancer; estrogen receptor; ESR1 mutations; endocrine resistance; CDK7 inhibition

Introduction

As the major driver of breast cancer development and progression, estrogen receptor- α (ER) is the pre-eminent target in 80% of breast cancers. Inhibition of ER activity with anti-estrogens or aromatase inhibitors (AI) for preventing estrogen biosynthesis, reduces relapse and improves patient survival^{9, 39}. However, in many patients tumours progress on these therapies, where resistant tumours are mostly ER-positive and frequently responsive to changes in endocrine agent^{1, 3, 22, 40}, although typically with shorter periods of response to second and third line endocrine treatments. Efforts to identify changes in ER that functionally act in resistance have shown that mutations in the ER gene are rare in primary breast cancer^{18, 38, 49}. However, new findings conclusively demonstrate that the ER gene (ESR1) is frequently mutated in advanced breast cancer; combining data from different reports indicates that ESR1 coding region mutations feature in about 20% of AI resistant breast cancer^{21, 34, 42, 45, 54}. The rarity of ESR1 mutations in primary breast cancer, as well as the lack of ESR1 mutations in matched primary samples from patients in which ESR1 mutations are evident after progression on endocrine therapies, indicates that treatment-selective pressures are likely to drive the acquisition of ESR1 mutations. Recent analyses of circulating tumour DNA further supports treatment-selective acquisition of ESR1 mutations^{16, 48}, and droplet digital PCR has identified ESR1 mutations in a proportion of primary tumours at very low mutant allele frequencies⁵⁶, suggesting that endocrine treatments may lead to selection of cancer cells with pre-existing ESR1 mutations.

The great majority of the mutations identified in advanced breast cancer occur in the ER ligand binding domain (LBD), with a “hotspot” at the consecutive amino acids L536, Y537 and D538, which map to the loop connecting α -helices 11 and 12. Structural analyses indicate that these residues control the agonist state of the LBD and that their mutation stabilizes the receptor in the agonist state, to promote co-activator recruitment^{4, 12} and thus aid transcription of ER target genes. Functional studies following ectopic expression of ER in which L536 or Y537 were substituted by other amino acids showed ligand-independent activation of estrogen-responsive reporter genes and interaction with co-activator proteins^{10, 11, 45, 59, 60, 63, 64}. Although ER mutated at these residues is inhibited by anti-estrogens, there is evidence for an attenuated response to anti-estrogens, at least for some substitutions^{21, 27, 54}. However, it is possible that the observed resistance is reflective of the fact that studies to date have employed ectopic over-expression of the mutant proteins.

CRISPR-Cas9 mediated genome editing provides a highly specific method for gene deletion and knockin mutagenesis in mammalian cells³¹, potentially allowing more faithful evaluation of the functional importance of gene mutations in model systems. Thus, CRISPR-Cas9 mediated introduction of mutations in the genomically encoded ESR1 gene would facilitate direct comparison of isogenic wild-type and mutant breast cancer cells towards developing a better understanding of the consequences of these mutations on response to

endocrine therapies, and importantly, would enable evaluation of therapeutic approaches to target breast cancers featuring ESR1 mutations. Toward this end, we have targeted Y537, the most frequently mutated ER residue, in the estrogen-responsive and anti-estrogen sensitive MCF7 cells. In MCF7 cells with a genomically encoded ER-Y537S mutation, we show ligand-independent recruitment of ER and regulation of gene expression in the absence of estrogen. Moreover, these cells grow in the absence of estrogen and show evidence of resistance to anti-estrogens.

Transcription regulation by ER requires cyclical association and dissociation from regulatory regions of target genes, in a process that is intimately linked with proteasomal degradation^{35, 44}. Phosphorylation of ER at Ser118 in the N-terminal transactivation function-1 (AF-1) plays a key role in ER recycling, by promoting interaction with the E3 ubiquitin ligase E6AP55. The importance of Ser118 phosphorylation is underscored by an association between Ser118 phosphorylation and response to endocrine therapy⁵¹. Moreover, P-Ser118 levels are elevated in tamoxifen-resistant breast cancer⁴⁷, implicating Ser118 phosphorylation in endocrine resistance. Estrogen binding results in recruitment of the basal transcription factor TFIID through a direct interaction with the ER LBD to promote Ser118 phosphorylation by the cyclin-dependent kinase (CDK)7 kinase of TFIID^{7, 8}. We show that CDK7 inhibition is effective in blocking growth of MCF7 ER-Y537S cells, demonstrating the utility of CRISPR-Cas9 generated breast cancer models of ER mutations for evaluating new therapeutic approaches for endocrine resistant breast cancer.

Materials and Methods

Cell culture and growth assays

MCF7-luc and MCF7-Y537S cells were authenticated by LGC Standards (UK) as being MCF7 derived and were routinely checked, and found to be negative, for mycoplasma infection. Cell lines were routinely cultured in DMEM containing 10% FCS. For estrogen depletion experiments, the cells were transferred to DMEM lacking phenol red and containing 5% dextran-coated charcoal-stripped FCS (DSS) for 72 hours. 17 β -estradiol (E2), 4-hydroxytamoxifen (OHT) and Faslodex (FAS) (Sigma-Aldrich, UK), were prepared in ethanol. THZ1 (ApexBio, USA), was dissolved in DMSO. Cell growth was assessed using the SRB assay⁵⁰. Briefly, 4,000 cells per well were seeded as six well technical replicates in 96-well plates in DMEM supplemented with 10% DSS. Sixteen hours later, the medium was replaced with fresh medium supplemented with E2, anti-estrogens, or an equivalent volume of the vehicle (ethanol). Medium was changed every 3 days and growth statistically analysed, so as to show average growth, with error bars for the Standard Error of the Mean (SEM). Each growth experiment was independently confirmed using three biological replicates.

CRISPR-Cas9 mediated generation of the MCF7-Y537S cell line

The ESR1 Y537S mutation was generated in MCF7-luc cells (Cell Biolabs Inc, USA) using CRISPR058819 (5'-GGCTAGTGGGCGCATGTAGG-3'), identified from the Human exon specific CRISPR database (http://arep.med.harvard.edu/human_crispr) and cloned into a guide-RNA expression plasmid (a gift from George Church; Addgene #41824), as

described³². For homologous recombination, a 1803 bp fragment of the ESR1 gene flanking the Exon 8 coding region was amplified using the primers 5'-GGAAGAGCTTGGAGACATGG-3' and 5'-AGGGCTAAATGCAACACCAG-3', from MCF7-luc genomic DNA and cloned into pJET1.2/blunt (Thermo Scientific UK). This ESR1 gene targeting template was modified by site-directed mutagenesis to incorporate a coding change for the Y537S mutation (TAT>TCT) and a silent "tagging" change at the codon for residue L536 (CTG>CTC). Site-directed mutagenesis generated additional silent mutations spanning the codons for residues 547-550, to prevent CRISPR058819-Cas9 mediated cleavage of the donor DNA. These changes also enable specific detection of Exon 8 targeted DNA by PCR with the mutation specific primer 5'-TAGTGGGCGCGTGAAGTCTA-3' and a second primer, 5'AAAATCAGTGTGGCTCCGGA-3', so as to generate a 712bp knockin specific PCR product, originating in genomic DNA 42nt upstream of the 5' end of the donor DNA.

ESR1 Exon 8 gene targeting plasmid, CRISPR058819 expression plasmid and the hCas9 expression plasmid (a gift from George Church; Addgene plasmid #41815) were co-transfected into MCF7-luc cells using an Amaxa Type II nucleofactor (Lonza, Germany). Following nucleofection, cells were allowed to grow in hormone-depleted culture medium, and established colonies subsequently expanded in DMEM supplemented with 10% FCS. Colonies were screened with the knockin-specific PCR and subsequently further characterised by DNA sequencing of a 462bp PCR product generated using primers with the sequences 5'-CCAGCTCCCATCCTAAAGTG-3' and 5'-TTGGCTAAAGTGGTGCATGA-3', which amplify the coding region of Exon 8.

Immunoblotting and immunoprecipitations

Whole cell lysates were prepared in RIPA buffer (Sigma-Aldrich, UK), supplemented with protease and phosphatase inhibitor cocktails (Roche, UK), as described². Immunoblotting was performed for two biological replicates, using 20 µg protein lysate. Immunoprecipitations for two biological replicates were carried out as as described⁴¹. Antibodies are detailed in supplementary table 1.

Liquid chromatography Mass Spectrometry (LC-MS)

Following immunoprecipitation of ER from MCF7 and MCF7-Y537S cells, ER on the beads was incubated overnight at 37C with trypsin in 1 M urea, in a total volume of 20 µl. After addition of 5 µl of 20% formic acid, spectra were generated by collision-induced dissociation of tryptic digests in the linear ion trap of the LTQ Orbitrap Velos instrument.

RNA preparation, quantitative RT-PCR and RNA-seq

Total RNA from three biological replicate cultures for each condition was extracted as previously described²⁶, with DNase treatment to remove genomic DNA. Quantitative RT-PCR (RT-qPCR) was carried out using three technical replicates for each sample for Taqman Gene Expression Assays (Applied Biosystems, UK), as listed in Supplementary Table 1 and presented as mean fold difference to the control, with error bars for SEM. RNA-seq was performed as described³⁷.

Chromatin Immunoprecipitations and Solexa sequencing (ChIP-seq)

MCF7 and Y537S cells were cultured in hormone-depleted medium for 72 hours. Chromatin was prepared from two biological replicates 45 minutes after addition of 10 nM estrogen and ChIP assays were performed as described⁴¹ using three technical replicates and the results compared using the unpaired t-test method. ChIP-seq was carried out on a single replicate for each treatment, using methods that have been described⁴¹.

Bioinformatic analyses

ChIP-seq analysis was as described⁴¹. RNA-seq data were analysed as described³⁷. In brief, paired-end 100bp reads, generated on an Illumina HiSeq 2500, were aligned using TopHat 2.0.14 and aligned reads were counted by HTSeq 0.6.1. The R package ‘DESeq2’ was used to normalize counts using a regularized log transformation (rlog)³⁰. Shrunken log₂ fold changes were also calculated to determine differentially expressed genes (DEGs) between conditions, while minimizing the fold change variation of low expression genes. Heat maps were generated in R using ‘gplots’ with rlog transformed read counts of DEGs. GSEA analysis was performed with the Molecular Signatures Database “Hallmarks” gene set collection²⁸.

The Binding and Expression Target Analysis (BETA) package⁵⁷ was used for integrating ChIP-seq and RNA-seq data. To identify direct ER target genes, BETA basic was run with a modified setting (look for peak within 100kb from gene transcription start site).

RNA-seq and ChIP-seq data have been deposited with the NCBI Gene Expression Omnibus (GEO) (<http://ncbi.nlm.nih.gov/geo/>) under accession number GSE78286.

Results

CRISPR-Cas9 mediated generation of MCF7 cells with a genomically encoded Y537S mutation in the ESR1 gene

Searching a human exon CRISPR database³² identified four potential CRISPR sequences that target exon 8 of the ESR1 gene proximal to the Y537 codon. To identify the most appropriate CRISPR sequence, we assessed the activities of each CRISPR in the HCT116 cell line, which has been widely used for creating gene knockouts. Sanger sequencing of genomic DNA prepared 96 hours after co-transfection of HCT116 cells showed that all four CRISPRs promoted indels, with CRISPR058819 being apparently the most efficient (Supplementary Fig. 1). This screening approach provides a rapid method for evaluating CRISPR activity and on this basis CRISPR058819 was used for generating the Y537S mutation in MCF7 cells.

Donor DNA for gene targeting consisted of a cloned 1.8 kb fragment of the ESR1 gene, flanking the Exon 8 coding region. This was mutated to generate the Y537S mutation (TAT>TCT), together with a silent, single base change in the L536 codon (CTG>CTC) and several silent changes to destroy the CRISPR058819 PAM recognition sequence (Supplementary Fig. 2A,B). The latter substitutions prevent CRISPR targeted cleavage of the donor template DNA by Cas9, provide a “tag” that distinguishes targeted from any

endogenously generated ESR1 exon 8 mutations and assist with specific PCR screening for the MCF7-Y537S mutation.

Following co-transfection of MCF7 cells with the donor template, CRISPR058819 and hCas9 plasmids, single colony cloning and PCR screening were used to isolate MCF7 cells with the ER-Y537S mutation. PCR of genomic DNA prepared from expanded clones with CRISPR058819 target site mutant-specific PCR primers identified positive clones, which were confirmed with DNA sequencing. Interestingly, of 6 clones with successful knockin mutations, all but one clone (MCF7-Y537S [NF2-A4]) featured indels which caused frameshift mutations in the second allele. Clones with indels were excluded from further analysis because of the potential for truncated ER proteins. DNA sequencing of the MCF7-Y537S [NF2-A4] (hereafter referred to as MCF7-Y537S) genomic DNA was consistent with a heterozygous line with one mutant allele (Supplementary Fig. 2C). RT-PCR of exons 5-8 with a primer that specifically amplifies the mutant allele (primer 2) gave a product only for MCF7-Y537S cells (Fig. 1B). The RT-PCR products for primers 1/3 were similar for both wild-type and MCF7-Y537S RNA. Sanger sequencing of the latter PCR product showed expression only of wild-type and Y537S mutant ER in MCF7-Y537S cells (Fig. 1C). Note that the smaller PCR product, which is consistent in size with an alternatively spliced ER mRNA lacking exon 7 sequences, has been described previously¹⁸. The exon-7 deleted mRNA is present at similar levels in both lines, suggesting that introduction of the Y537S mutation does not alter ER gene expression patterns. Quantification of RNA-seq reads confirmed that the MCF7-Y537S line expresses only wild-type and Y537S mutant ER mRNA (Fig. 1D). To demonstrate that MCF7-Y537S cells express the mutant protein, ER was immunoprecipitated and immunoprecipitates were analysed by LC-MS following tryptic digestion. A tryptic peptide corresponding to wild-type, but not mutant ER, was detected in MCF7 cells (Fig. 1E, Supplementary Fig. 2D). In MCF7-Y537S cells, both peptides were detected, with levels of wild-type and mutant peptides being similar in each replicate. This further confirms similar levels of expression for both ER proteins in MCF7-Y537S cells.

MCF7-Y537S cells grow in the absence of estrogen and are partially resistant to anti-estrogens

Whereas MCF7-WT growth was estrogen-dependent, growth of MCF7-Y537S cells was similar in the presence or absence of estrogen and comparable to that of estrogen-treated MCF7-WT cells (Fig. 2A). In the absence of estrogen, OHT inhibited growth of MCF7-Y537S cells in a dose-dependent manner (Fig. 2B), but complete growth inhibition was only achieved for 1 μ M OHT (3.7 fold). To investigate the effects of OHT in the presence of estrogen, the cells were treated with increasing doses of OHT in the presence of 10 nM estrogen. MCF7 cell growth was inhibited 2.8 fold at 1 μ M OHT, this being comparable to the minimal growth seen in estrogen-depleted medium. By contrast, even with 1 μ M OHT, growth of MCF7-Y537S growth was only modestly repressed (1.4 fold inhibition).

FAS was a more effective inhibitor of MCF7-Y537S growth (Fig. 2C). As can be seen, only 1 μ M FAS was effective at inhibiting MCF7-WT cell growth in the presence of 10 nM estrogen, where it led to a 4.3 fold inhibition of estrogen stimulated growth, this being

comparable to growth for this line in estrogen deprived medium. MCF7-Y537S cells were similarly growth inhibited by 1 μ M FAS in the presence of 10 nM estrogen, this causing a 4.1 fold inhibition of the growth seen in 10 nM estrogen alone. For MCF7-Y537S cells, all concentrations of FAS tested inhibited the potent growth of this line in the absence of estrogen, with 10 nM - 1 μ M FAS leading to a 5.5-6.5 fold inhibition.

In full medium conditions (Fig. 2D), MCF7-WT cells showed a titratable response to OHT, with growth in 1 μ M OHT being inhibited by 1.5 fold over the untreated cells. In contrast, growth of the MCF7-Y537S line was unaffected by OHT. Under full medium conditions, MCF7-WT cells also showed potent growth inhibition by FAS over the range 1 nM -1 μ M, with 10 nM – 1 μ M FAS resulting in >3 fold inhibition over untreated cells. The response to FAS by the MCF7-Y537S line under the same conditions was less pronounced, with 10nM FAS showing only a 1.2 fold inhibition, but growth was inhibited fully with 1 μ M FAS (2.6 fold over vehicle treated cells; Fig. 2D).

Taken together, these findings provide evidence that breast cancer cells harboring single allele ER-Y537S mutations, acquire both a resistance to anti-estrogens and a capacity to grow efficiently under estrogen-depleted conditions.

ER-Y537S is recruited to ER binding regions in an estrogen-independent manner to promote co-activator recruitment and histone modification

The above findings suggest that the ER-Y537S mutation promotes estrogen-independent expression of ER target genes. Towards addressing this directly, we performed ER ChIP-seq (Supplementary Fig. 3). Peak calling identified 5,930 and 22,088 ER binding sites in MCF7 cells in the absence and presence of estrogen, respectively. By contrast, there were 11,092 ER binding regions in vehicle treated MCF7-Y537S cells, most of which were shared with estrogen treated MCF7-Y537S (88% (9,743/11,092)) and MCF7-WT (77% (8,510/11,092)) cells (Fig. 3A). Additional peaks were called for estrogen-treated MCF7-Y537S cells, which were also present in estrogen-treated MCF7 cells. A heat map comparison of ER binding events between the lines showed that the binding profiles in unstimulated Y537S cells is similar to that seen in estrogen-induced MCF7 cells (Fig. 3B), as demonstrated in plots of average peak profiles, which showed a considerably greater magnitude of ER binding in the absence of estrogen in MCF7-Y537S, than in WT cells (Fig. 3C), as exemplified for the TFF1 and XBP1 genes (Fig. 3C). Motif enrichment analysis did not suggest that the Y537S mutation causes ER binding to new sites (Fig. 3E; Supplementary Table 2). In all conditions, the most enriched binding motifs were the ER binding site (ERE), followed by FOXA1, AP-1 and GATA3 binding sites.

ChIP-qPCR confirmed ER recruitment in an estrogen-independent manner in MCF7-Y537S cells (Fig. 3F). Recruitment of the transcriptional coactivators AIB1 and p300, was also estrogen-independent (Fig. 3G, H). Histone H3 acetylation and RNA polymerase II (PolII) were also elevated at ER binding regions in MCF7-Y537S cells in the absence of estrogen (Fig. 3I, J), suggestive of estrogen-independent transcription in this line. FOXA1 recruitment was unaffected by the Y537S mutation (Fig. 3K), which is in keeping with its described role as a pioneer factor that pre-exists at ER binding regions and which acts to direct ER recruitment to chromatin²³.

ER target gene expression is ligand-independent and is frequently enhanced in MCF7-Y537S cells

To determine the consequence of the Y537S mutation on ER target gene expression, we performed RNA-seq for MCF7 and MCF7-Y537S cells. Treatment of cells with estrogen for 8 hours was chosen following evaluation of the expression of well-known ER target genes in a time course of estrogen treatment (Supplementary Fig. 4A). This time point showed robust stimulation of ER target gene expression in MCF7 cells, but would be expected to show limited estrogen stimulation of indirect targets. For each condition, three independent replicate samples were analysed by RNA-seq. Analysis with the RNASeqPower package in R for our data showed that three replicates gave a power >0.8 for a fold change of 1.5. As the sequencing data for one of the three replicates for MCF7-Y537S cells treated with estrogen failed quality control, two data sets were available for analysis. In MCF7 cells, 4,873 genes were differentially regulated by treatment with estrogen ($\text{padj}<0.05$; Fig. 4A). Comparison of vehicle treated MCF7 and MCF7-Y537S cells showed that the majority (75%; 3,657/4,873) of genes that are estrogen-regulated in MCF7 cells are differentially regulated in MCF7-Y537S cells. Of these genes, only 31% (1,141/3,657) are estrogen regulated in MCF7-Y537S cells (see also supplementary Fig. 4B), suggesting that most estrogen-responsive genes are ligand-independent in MCF7-Y537S cells. Gene set enrichment analysis (GSEA) identified pathways including early and late estrogen responsive targets (Fig. 4B; Supplementary Table 3). Also enriched were pathways associated with cell proliferation, including E2F and Myc targets and the G2M checkpoint. Interestingly, several GSEA pathways enriched with estrogen treatment of MCF7 cells remained estrogen-regulated in MCF7-Y537S cells. For the most part, these were pathways that were down-regulated in estrogen treated MCF7 cells and included protein secretion, heme metabolism and apoptosis. There was also the suggestion of further augmentation of ER regulated gene expression in the presence, compared with the absence of estrogen in MCF7-Y537S cells, which is in agreement with the estrogen-stimulated ER recruitment observed for the MCF7-Y537S ER ChIP-seq.

Analysis of the differentially regulated genes using RNASeqPower, indicated a fold change cut-off >1.5 was required for power >0.8 . 5,407 genes were differentially regulated with $\text{FC}>1.5$ and $\text{padj}<0.05$. Hierarchical cluster analysis of the differentially regulated genes showed segregation in two large clusters; genes that showed estrogen stimulation in MCF7 cells and the expression of which was elevated in MCF7-Y537S cells and a second group comprising genes whose expression was reduced in estrogen-treated MCF7 cells and which were further repressed in MCF7-Y537S cells (Supplementary Fig. 4C).

To examine regulation of direct ER target genes, we integrated the ER ChIP-seq data with the estrogen responsive genes in MCF7 cells ($\text{padj}<0.05$ from RNA-seq, above), using the Binding and Expression Target Analysis (BETA) package⁵⁷. ChIP-seq and RNA-seq integration identified 1,559 genes with an ER peak within 100 kb of transcription start sites. Hierarchical cluster analysis of the RNA-seq data for these genes identified four main groups (Fig. 4C; Supplementary Table 4). Cluster 1 comprised genes whose expression is stimulated by estrogen in MCF7 cells. Expression of genes in this cluster was elevated in vehicle-treated MCF7-Y537S cells and was further increased with estrogen treatment. Genes

in this cluster include well-characterised ER target genes, such as PGR, TFF1, CTSD, GREB1, NRIP1, XBP1, EGR3, CA12, PDZK1, IGFR, AREG and H19. As many genes are repressed by estrogen in breast cancer cells, as are stimulated¹⁴ and cluster 4 incorporates genes that are repressed by estrogen in MCF7 cells. Expression of cluster 4 genes was generally lower in MCF7-Y537S cells than in vehicle treated MCF7 cells and was further reduced in estrogen treated MCF7-Y537S cells. This is exemplified by ERBB2 (ref²⁰), the expression of which was 0.8-fold in estrogen treated, compared with vehicle treated MCF7 cells and was reduced to 0.7- and 0.6-fold in vehicle and estrogen treated MCF7-Y537S (Supplementary Table 4). The other two clusters include genes whose expression is estrogen-stimulated and -repressed in MCF7 cells. Genes in these two clusters exhibited reduced estrogen responsiveness in MCF7-Y537S cells; expression in the absence of estrogen was similar to expression levels in vehicle-treated MCF7 cells.

40% of the genes that were differentially regulated between MCF7 and MCF7-Y537S cells were estrogen regulated in MCF7 cells and, as described above, are likely to mainly constitute direct ER target genes. The remaining differential genes may be involved in signalling pathways downstream of direct ER targets. To assess this, we analysed RNA-seq data for MCF7 which were cultured long-term in full medium³⁷. Most of the genes whose expression was altered following 8 hours estrogen treatment in MCF7 cells, were identified in vehicle-treated MCF7-Y537S and in MCF7 cells cultured in full medium (2884 genes; Supplementary Figure 5A). Indeed, “estrogen response early” was the most significantly enriched GSEA pathway in this gene set (Supplementary Figure 5B). Of the remaining genes identified in MCF7-Y537S cells, the majority (~70%), are also observed for the full medium conditions. This set of genes were enriched in signaling pathways associated with the G2M checkpoint and mitotic spindle, as well as metabolic pathways including fatty acid metabolism, oxidative phosphorylation and glycolysis (Supplementary Figure 5C). Analysis of an independent RNA-seq study where MCF7 cells were cultured in estrogen-depleted medium and treated with estrogen for 24 hours²⁹ gave very similar results (Supplementary Figure 5D-F). Together, these analyses show that estrogen regulated gene expression is a dominant feature that defines the MCF7-Y537S transcriptome.

To validate the RNA-seq findings, we focused on genes in cluster 1, as these include many of the best characterised ER target genes in breast cancer. In hormone-depleted MCF7-Y537S cells, mRNA levels of these genes were high in the absence of estrogen, at levels similar to those observed for estrogen-treated WT cells (Fig. 4D). As observed for RNA-seq, expression of most genes was further stimulated by estrogen in MCF7-Y537S cells, to levels considerably higher than those achieved in estrogen-treated WT cells. Particularly striking is PGR, mRNA levels of which were 3.3- and 7.6-fold higher in the absence and presence of estrogen, respectively, compared with PGR expression in estrogen-treated MCF7 cells. This was reflected in the remarkably elevated levels of both PGR isoforms, PGR-A and PGR-B, in MCF7-Y537S cells, compared with WT cells (Fig. 4E). In full medium conditions, expression of these ER targets was also elevated in MCF7-Y537S mutant, compared with WT MCF7 cells (Supplementary Fig. 6A).

Treatment with 10 nM OHT or FAS inhibited expression of these genes; nevertheless expression of most genes was higher than that in anti-estrogen treated WT cells. Indeed,

whereas expression of PGR, TFF1 and CTSD was inhibited by as little as 1 nM OHT, levels of these proteins remained high even in the presence of 1 μ M OHT (Supplementary Fig. 6B). ER target gene expression was more responsive to FAS, but as for OHT, levels of all proteins were higher in the FAS treated MCF7-Y537S cells than in parental MCF7 cells (Supplementary Fig. 6C).

Finally, our results show that ER mRNA levels were similar in MCF7-WT and MCF7-Y537S cells (Fig. 4D). Previous studies have shown that ER protein levels are reduced upon treatment of MCF7 cells with estrogen, OHT stabilises ER and FAS promotes ER degradation (e.g. see61). In agreement, ER protein levels were elevated with OHT treatment and were reduced by FAS treatment in MCF7 cells (Fig. 4E, Supplementary Fig. 6B-C). ER levels showed similar ligand regulation in MCF7-Y537S cells, which suggests that ER binding to ligands and its stability are not substantially affected by the Y537S mutation.

CDK7 directed Ser-118 phosphorylation is ligand-independent in MCF7-Y537S cells

Estrogen binding promotes an interaction between the TFIID complex that is mediated by the ER LBD and α -helical LXXLL motifs in the XPD and p62 subunits of TFIID, resulting in Ser118 phosphorylation by the TFIID kinase CDK7 (ref.7). TFIID co-immunoprecipitated with ER in the presence, but not the absence of estrogen, as shown by immunoblotting for the XPD subunit of TFIID (Fig. 5A). In MCF7-Y537S cells, ER interacted with XPD in an estrogen-independent manner. Moreover, Ser118 phosphorylation was ligand-dependent in MCF7 cells, but was constitutive in MCF7-Y537S cells (Fig. 4E).

THZ1 is a selective inhibitor of CDK7 that has demonstrable anti-tumour activities for a wide range of cancer types²⁴, acting to inhibit transcription by preventing phosphorylation of the RNA polymerase II (PolII) C-terminal domain heptapeptide repeats, and affecting cell cycle progression by inhibiting CDK7-mediated phosphorylation of CDK1, CDK2, CDK4 and CDK6 (ref.13). THZ1 inhibited MCF7 cell growth (GI_{50} =188 nM) (Figure 5B). MCF7-Y537S cells were slightly more sensitive to THZ1 (GI_{50} =162 nM), albeit with a difference that was not statistically significant. Inhibition of growth was accompanied by dose-dependent inhibition of PolII CTD phosphorylation (Fig. 5C).

Reasoning that since (a) ER is a transcriptional driver in breast cancer cells, (b) CDK7 activity is required for transcription and (c) CDK7 phosphorylates ER at Ser118, we determined if co-treatment with THZ1 and anti-estrogens would provide additional growth inhibition. THZ1 augmented MCF7-Y537S inhibition by 10 nM FAS (Fig. 5D). For 100 nM FAS, MCF7-Y537S growth was completely suppressed when combined with 75 nM THZ1. PolII phosphorylation was unaffected by FAS, being inhibited entirely by THZ1 (Fig. 5E). RB phosphorylation was inhibited in a dose-dependent manner by FAS and was further inhibited by THZ1 co-treatment (Fig. 5F). There was also a dose-dependent inhibition of Ser118 phosphorylation by FAS and strong inhibition by THZ1 (Fig. 5G). Moreover, repression of ER target genes, PGR and RARA was greatest for the FAS/THZ1 combination. An important part of the response to THZ1 appears to derive from the special sensitivity of cancer cells to transcriptional inhibition of key driver genes, as exemplified in T-cell acute lymphoblastic leukemia cells (T-ALL)²⁴. RUNX1, TAL1 and GATA3, which together constitute a critical transcriptional circuit in T-ALL, were amongst the genes that were most

sensitive to THZ1. Interestingly, GATA3 was strongly inhibited by THZ1 in MCF7 and MCF7-Y537S cells. As a pioneer factor for ER in breast cancer cells⁵³, the potent inhibition of GATA3 expression provides further evidence for its potential utility in the treatment of ER-positive breast cancer.

Discussion

Mutations in the ER gene have recently been found to be common in advanced breast cancer and are likely to represent an important mechanism of endocrine resistance. Understanding the impact of these mutations on ER signaling in breast cancer cells is a crucial step towards identifying therapeutic interventions following emergence of ER mutations. Although tumour explants and patient-derived xenografts (PDX) will be important for testing alternative therapies, modeling them in established, well-characterised breast cancer cell lines should facilitate rapid and intensive evaluation. By facilitating the generation of isogenic lines with mutations of interest encoded within endogenous genes, the application of CRISPR-Cas9 methodologies for gene replacement promises a powerful new tool for bypassing problems inherent in over-expression studies. With this in mind, we replaced tyrosine 537 in the endogenous ER gene of MCF7 estrogen responsive breast cancer cells, to make serine 537, one of the most common ER mutations in advanced, metastatic breast cancer.

Sequencing of genomic DNA, RNA-seq and quantitative mass-spectrometry demonstrated that MCF7-Y537S cells encode one copy of the mutant allele and express wild-type and Y537S ER proteins at equivalent levels, as is likely in metastatic breast cancer. This was sufficient to drive estrogen-independent growth, indicating that the Y537S mutation is dominant. Recently, Fanning et al¹² have reported detailed ligand binding properties of the Y537S LBD. Using a radioligand binding assay, they found that the affinity of E2 for the wild-type LBD is five-fold greater than that seen for the Y537S LBD. Further, while, X-ray crystallography analysis of the apo- and agonist-bound states of the Y537S LBD show near identical helix 12 conformations, equating to a stable agonist state in the absence of E2, time-resolved Forster Resonance Energy Transfer (tr-FRET) measurements of coactivator binding show that E2 results in an increase in coactivator affinity in the Y537S LBD. Indeed, this behaviour is likely to be an important factor in both the E2 response of MCF7-Y537S cells, when comparing the expression of estrogen regulated genes between mutant and wild-type cells, and the mechanisms underlying the resistance to antiestrogens exhibited by MCF7-Y537S cells.

MCF7-Y537S cells were found to be resistant to both tamoxifen and the ER downregulator faslodex, although resistance to faslodex was less pronounced. In estrogen-free conditions, MCF7-Y537S cells were strongly inhibited by 1 and 10 nM FAS. However, if estrogen was present, potent growth inhibition required 100 nM FAS. It should be noted that peak (C_{max}) plasma concentrations in patients following high dose administration of faslodex (500 mg), average at about 20 ng/ml (approximately 30 nM)^{33, 43}, suggesting that only partial inhibition of ER signaling may be achievable with faslodex in patients with the Y537S mutation.

Using a competitive radioligand-binding assay to determine the relative binding affinities of OHT for WT and Y537S mutant LBDs, Fanning et al¹² found that binding to the mutant LBD was 8-10 fold weaker than to the WT. Further, expression of Y537S mutated ER in the ER positive T47D breast cancer cell line has shown that FAS can downregulate endogenous WT and transfected mutant ER protein, and could partially suppress growth of the mutant-expressing cells. Both the greatly reduced binding affinity of ER-Y537S to OHT, and the continued sensitivity of the mutant receptor to FAS, are consistent with the response that our MCF7-Y537S cells exhibit to anti-estrogens. It is possible that new selective estrogen receptor modulators, such as the orally bioavailable AZD9496, GDC-0810 and RAD1901, could improve on patient responses, since they may not be subject to the dose limitations due to the poor pharmaceutical properties of fulvestrant^{15, 25, 58}. Additionally, we have now shown that it may be possible to achieve CDK7 inhibitor promoted growth inhibition using clinically achievable fulvestrant doses.

Of the group of ER LBD coding mutations featured in breast cancer, mutations of tyrosine 537 are amongst the most prevalent, with the Y537S mutation being the most frequent of these. It is well established that tyrosine 537 is the major tyrosine phosphorylation site in ER, where it is involved in receptor dimerisation and DNA binding^{5, 6}. Furthermore, it has been shown that the Y537S mutated receptor also dimerises effectively⁶². Intriguingly, recent studies employing a chemical semi-synthesis strategy to prepare site specific *in vitro* phosphorylated ER LBDs have shown that tyrosine 537 phosphorylation results in a ligand-independent increase in coactivator binding⁵². The activity of the Y537S ER mutation in this context similarly needs to be studied in detail, so that a better understanding of this mutation in metastatic breast cancer can be achieved. Clearly, the genome engineered MCF7-Y537S line described in our study provides an appropriate cellular model in which the findings from such studies can be evaluated and, perhaps more importantly, could be further used to develop new therapeutic strategies for metastatic breast cancer featuring Y537S ER mutations.

Mapping global ER binding showed that the Y537S mutation promotes estrogen-independent ER recruitment. Furthermore, recruitment of co-activators including AIB1 and p300, as well as PolII, was increased in the absence of estrogen. ER, co-activator and PolII recruitment were stimulated by estrogen, presumably due to co-expression with wild-type ER and/or estrogen stimulation of ER-Y537S activity. The majority (63%) of genes whose expression was stimulated by estrogen in MCF7 cells, were upregulated in MCF7-Y537S cells in the absence of estrogen. Expression of these genes was stimulated further by estrogen. Estrogen treatment of MCF7 cells represses expression of as many, or more, genes than are stimulated¹⁴. Integration of ER ChIP-seq and RNA-seq data identified 1,559 estrogen regulated genes in MCF7 cells, of which 52% were repressed by estrogen. Interestingly, the majority (65%) of these genes were repressed in MCF7-Y537S cells in the absence of estrogen and were further repressed by estrogen. These analyses indicate that the Y537S mutation does not reprogramme ER by causing genomic redistribution of ER or expression of new target genes, confirmed by the fact that GSEA analysis did not provide evidence for new signaling pathways.

The considerable over-expression, or “super-induction” of the majority of estrogen-induced genes is extremely interesting and deserves further investigation. As expression of many transcription factors that co-operate with ER, such as RARA, PGR, LRH-1 and c-myc, as well as many transcriptional coregulators, including AIB1, NRIP1, is stimulated by ER activation, estrogen-independent expression of these factors might be important for promoting chromatin remodelling and enhanced transcription at ER target genes. Gene expression at ER target genes requires the co-ordinated and cyclical recruitment and dissociation of ER and co-regulators at ER target genes³⁵. Ligand-independent recruitment of ER, and up-regulation of ER regulated transcription factors and co-regulators might alter the kinetics of chromatin remodelling, towards greater gene transcription. Also unexpected was the finding that the expression of many ER target genes was not ligand-independent, and indeed expression of many ER target genes, as evidenced by genes in clusters 2 and 3, was blunted in MCF7-Y537S cells. At present we can only speculate that these classes of genes involve co-operativity of ER with additional/alternative factors that are themselves estrogen regulated. Determination of ER and co-factor recruitment and chromatin modification/remodelling in time course studies of genes representative of the different categories, as well as proteomic approaches for identifying factors recruited to ER binding regions in MCF7 and MCF7-Y537S cells would help to more clearly define the mechanisms at work.

Notwithstanding, our results raise the possibility that tumours with ER mutations might be especially sensitive to drugs that target the activities of super-induced genes. Examples of strongly over-expressed genes identified by our analyses include RARA and PGR, for which agonists/antagonist drugs are available and both of which are key regulators of ER action in breast cancer^{19, 36, 46}. MCF7-Y537S cells provide an important vehicle for testing these and other therapeutic strategies, for example with genome-wide or targeted siRNA screening, or screening of drug libraries. Our results for the CDK7 inhibitor THZ1, exemplify such approaches for evaluation of new therapies that could be used singly, or in combination with endocrine therapies.

Supplementary Material

Refer to Web version on PubMed Central for supplementary material.

Acknowledgements

This work was funded by grants from Breast Cancer Now (2014MayPR234) and Cancer Research UK (C37/A18784). AH is supported by a PhD studentship from the Cancer Research UK Imperial Centre. We thank M Jones and L Game, MRC CSC Genomics Facility, Imperial College London. This study is dedicated to the memory of Professor Susan Malcolm.

References

1. Ali S, Coombes RC. Endocrine-responsive breast cancer and strategies for combating resistance. *Nat Rev Cancer*. 2002; 2:101–112. [PubMed: 12635173]
2. Ali S, Heathcote DA, Kroll SH, Jogalekar AS, Scheiper B, Patel H, et al. The development of a selective cyclin-dependent kinase inhibitor that shows antitumor activity. *Cancer Res*. 2009; 69:6208–6215. [PubMed: 19638587]

3. Ali S, Buluwela L, Coombes RC. Antiestrogens and their therapeutic applications in breast cancer and other diseases. *Annu Rev Med.* 2011; 62:217–232. [PubMed: 21054173]
4. Anghel SI, Perly V, Melancon G, Barsalou A, Chagnon S, Rosenauer A, et al. Aspartate 351 of estrogen receptor alpha is not crucial for the antagonist activity of antiestrogens. *The Journal of biological chemistry.* 2000; 275:20867–20872. [PubMed: 10787412]
5. Arnold SF, Vorojeikina DP, Notides AC. Phosphorylation of tyrosine 537 on the human estrogen receptor is required for binding to an estrogen response element. *The Journal of biological chemistry.* 1995; 270:30205–30212. [PubMed: 8530431]
6. Arnold SF, Melamed M, Vorojeikina DP, Notides AC, Sasson S. Estradiol-binding mechanism and binding capacity of the human estrogen receptor is regulated by tyrosine phosphorylation. *Mol Endocrinol.* 1997; 11:48–53. [PubMed: 8994187]
7. Chen D, Riedl T, Washbrook E, Pace PE, Coombes RC, Egly JM, et al. Activation of estrogen receptor alpha by S118 phosphorylation involves a ligand-dependent interaction with TFIIH and participation of CDK7. *Mol Cell.* 2000; 6:127–137. [PubMed: 10949034]
8. Chen D, Washbrook E, Sarwar N, Bates GJ, Pace PE, Thirunuvakkarasu V, et al. Phosphorylation of human estrogen receptor alpha at serine 118 by two distinct signal transduction pathways revealed by phosphorylation-specific antisera. *Oncogene.* 2002; 21:4921–4931. [PubMed: 12118371]
9. Cuzick J, Sestak I, Baum M, Buzdar A, Howell A, Dowsett M, et al. Effect of anastrozole and tamoxifen as adjuvant treatment for early-stage breast cancer: 10-year analysis of the ATAC trial. *Lancet Oncol.* 2010; 11:1135–1141. [PubMed: 21087898]
10. Eng FC, Lee HS, Ferrara J, Willson TM, White JH. Probing the structure and function of the estrogen receptor ligand binding domain by analysis of mutants with altered transactivation characteristics. *Molecular and cellular biology.* 1997; 17:4644–4653. [PubMed: 9234721]
11. Eng FC, Barsalou A, Akutsu N, Mercier I, Zechel C, Mader S, et al. Different classes of coactivators recognize distinct but overlapping binding sites on the estrogen receptor ligand binding domain. *The Journal of biological chemistry.* 1998; 273:28371–28377. [PubMed: 9774463]
12. Fanning SW, Mayne CG, Dharmarajan V, Carlson KE, Martin TA, Novick SJ, et al. Estrogen receptor alpha somatic mutations Y537S and D538G confer breast cancer endocrine resistance by stabilizing the activating function-2 binding conformation. *eLife.* 2016; 5
13. Fisher RP. Secrets of a double agent: CDK7 in cell-cycle control and transcription. *Journal of cell science.* 2005; 118:5171–5180. [PubMed: 16280550]
14. Frasar J, Danes JM, Komm B, Chang KC, Lyttle CR, Katzenellenbogen BS. Profiling of estrogen up- and down-regulated gene expression in human breast cancer cells: insights into gene networks and pathways underlying estrogenic control of proliferation and cell phenotype. *Endocrinology.* 2003; 144:4562–4574. [PubMed: 12959972]
15. Garner F, Shomali M, Paquin D, Lyttle CR, Hattersley G. RAD1901: a novel, orally bioavailable selective estrogen receptor degrader that demonstrates antitumor activity in breast cancer xenograft models. *Anticancer Drugs.* 2015; 26:948–956. [PubMed: 26164151]
16. Guttery DS, Page K, Hills A, Woodley L, Marchese SD, Rghebi B, et al. Noninvasive detection of activating estrogen receptor 1 (ESR1) mutations in estrogen receptor-positive metastatic breast cancer. *Clin Chem.* 2015; 61:974–982. [PubMed: 25979954]
17. Heinz S, Benner C, Spann N, Bertolino E, Lin YC, Laslo P, et al. Simple combinations of lineage-determining transcription factors prime cis-regulatory elements required for macrophage and B cell identities. *Mol Cell.* 2010; 38:576–589. [PubMed: 20513432]
18. Herynk MH, Fuqua SA. Estrogen receptor mutations in human disease. *Endocrine reviews.* 2004; 25:869–898. [PubMed: 15583021]
19. Hua S, Kittler R, White KP. Genomic antagonism between retinoic acid and estrogen signaling in breast cancer. *Cell.* 2009; 137:1259–1271. [PubMed: 19563758]
20. Hurtado A, Holmes KA, Geistlinger TR, Hutcherson IR, Nicholson RI, Brown M, et al. Regulation of ERBB2 by oestrogen receptor-PAX2 determines response to tamoxifen. *Nature.* 2008; 456:663–666. [PubMed: 19005469]
21. Jeselsohn R, Yelensky R, Buchwalter G, Frampton G, Meric-Bernstam F, Gonzalez-Angulo AM, et al. Emergence of constitutively active estrogen receptor-alpha mutations in pretreated advanced

- estrogen receptor-positive breast cancer. *Clinical cancer research: an official journal of the American Association for Cancer Research*. 2014; 20:1757–1767. [PubMed: 24398047]
22. Johnston SR, Dowsett M. Aromatase inhibitors for breast cancer: lessons from the laboratory. *Nat Rev Cancer*. 2003; 3:821–831. [PubMed: 14668813]
 23. Jozwik KM, Carroll JS. Pioneer factors in hormone-dependent cancers. *Nat Rev Cancer*. 2012; 12:381–385. [PubMed: 22555282]
 24. Kwiatkowski N, Zhang T, Rahl PB, Abraham BJ, Reddy J, Ficarro SB, et al. Targeting transcription regulation in cancer with a covalent CDK7 inhibitor. *Nature*. 2014; 511:616–620. [PubMed: 25043025]
 25. Lai A, Kahraman M, Govek S, Nagasawa J, Bonnefous C, Julien J, et al. Identification of GDC-0810 (ARN-810), an Orally Bioavailable Selective Estrogen Receptor Degradator (SERD) that Demonstrates Robust Activity in Tamoxifen-Resistant Breast Cancer Xenografts. *J Med Chem*. 2015; 58:4888–4904. [PubMed: 25879485]
 26. Lai CF, Flach KD, Alexi X, Fox SP, Ottaviani S, Thiruchelvam PT, et al. Co-regulated gene expression by oestrogen receptor alpha and liver receptor homolog-1 is a feature of the oestrogen response in breast cancer cells. *Nucleic Acids Res*. 2013; 41:10228–10240. [PubMed: 24049078]
 27. Li S, Shen D, Shao J, Crowder R, Liu W, Prat A, et al. Endocrine-Therapy-Resistant ESR1 Variants Revealed by Genomic Characterization of Breast-Cancer-Derived Xenografts. *Cell Rep*. 2013
 28. Liberzon A, Birger C, Thorvaldsdottir H, Ghandi M, Mesirov JP, Tamayo P. The Molecular Signatures Database (MSigDB) hallmark gene set collection. *Cell Syst*. 2015; 1:417–425. [PubMed: 26771021]
 29. Liu Y, Zhou J, White KP. RNA-seq differential expression studies: more sequence or more replication? *Bioinformatics*. 2014; 30:301–304. [PubMed: 24319002]
 30. Love MI, Huber W, Anders S. Moderated estimation of fold change and dispersion for RNA-seq data with DESeq2. *Genome Biol*. 2014; 15:550. [PubMed: 25516281]
 31. Mali P, Esvelt KM, Church GM. Cas9 as a versatile tool for engineering biology. *Nature methods*. 2013; 10:957–963. [PubMed: 24076990]
 32. Mali P, Yang L, Esvelt KM, Aach J, Guell M, DiCarlo JE, et al. RNA-guided human genome engineering via Cas9. *Science*. 2013; 339:823–826. [PubMed: 23287722]
 33. McCormack P, Sapunar F. Pharmacokinetic profile of the fulvestrant loading dose regimen in postmenopausal women with hormone receptor-positive advanced breast cancer. *Clin Breast Cancer*. 2008; 8:347–351. [PubMed: 18757262]
 34. Merenbakh-Lamin K, Ben-Baruch N, Yeheskel A, Dvir A, Soussan-Gutman L, Jeselsohn R, et al. D538G Mutation in Estrogen Receptor-alpha: A Novel Mechanism for Acquired Endocrine Resistance in Breast Cancer. *Cancer Res*. 2013
 35. Metivier R, Penot G, Hubner MR, Reid G, Brand H, Kos M, et al. Estrogen receptor-alpha directs ordered, cyclical, and combinatorial recruitment of cofactors on a natural target promoter. *Cell*. 2003; 115:751–763. [PubMed: 14675539]
 36. Mohammed H, Russell IA, Stark R, Rueda OM, Hickey TE, Tarulli GA, et al. Progesterone receptor modulates ERalpha action in breast cancer. *Nature*. 2015; 523:313–317. [PubMed: 26153859]
 37. Nguyen VT, Barozzi I, Faronato M, Lombardo Y, Steel JH, Patel N, et al. Differential epigenetic reprogramming in response to specific endocrine therapies promotes cholesterol biosynthesis and cellular invasion. *Nat Commun*. 2015; 6:10044. [PubMed: 26610607]
 38. Oesterreich S, Davidson NE. The search for ESR1 mutations in breast cancer. *Nat Genet*. 2013; 45:1415–1416. [PubMed: 24270445]
 39. Osborne CK. Tamoxifen in the treatment of breast cancer. *N Engl J Med*. 1998; 339:1609–1618. [PubMed: 9828250]
 40. Osborne CK, Schiff R. Mechanisms of endocrine resistance in breast cancer. *Annu Rev Med*. 2011; 62:233–247. [PubMed: 20887199]
 41. Periyasamy M, Patel H, Lai CF, Nguyen VT, Nevedomskaya E, Harrod A, et al. APOBEC3B-Mediated Cytidine Deamination Is Required for Estrogen Receptor Action in Breast Cancer. *Cell Rep*. 2015; 13:108–121. [PubMed: 26411678]

42. Piccart M, Rugo H, Chen D, Campone M, Burris AH, Taran T, et al. Assessment of genetic alterations in postmenopausal women with hormone receptor-positive, HER2-negative advanced breast cancer from the BOLERO-2 trial by next-generation sequencing. *J Clin Oncol.* 2013; 24:iii25–iii26.
43. Pritchard KI, Rolski J, Papai Z, Mauriac L, Cardoso F, Chang J, et al. Results of a phase II study comparing three dosing regimens of fulvestrant in postmenopausal women with advanced breast cancer (FINDER2). *Breast cancer research and treatment.* 2010; 123:453–461. [PubMed: 20632084]
44. Reid G, Hubner MR, Metivier R, Brand H, Denger S, Manu D, et al. Cyclic, proteasome-mediated turnover of unliganded and liganded ERalpha on responsive promoters is an integral feature of estrogen signaling. *Mol Cell.* 2003; 11:695–707. [PubMed: 12667452]
45. Robinson DR, Wu YM, Vats P, Su F, Lonigro RJ, Cao X, et al. Activating ESR1 mutations in hormone-resistant metastatic breast cancer. *Nat Genet.* 2013
46. Ross-Innes CS, Stark R, Holmes KA, Schmidt D, Spyrou C, Russell R, et al. Cooperative interaction between retinoic acid receptor-alpha and estrogen receptor in breast cancer. *Genes & development.* 2010; 24:171–182. [PubMed: 20080953]
47. Sarwar N, Kim JS, Jiang J, Peston D, Sinnott HD, Madden P, et al. Phosphorylation of ERalpha at serine 118 in primary breast cancer and in tamoxifen-resistant tumours is indicative of a complex role for ERalpha phosphorylation in breast cancer progression. *Endocrine-related cancer.* 2006; 13:851–861. [PubMed: 16954434]
48. Schiavon G, Hrebien S, Garcia-Murillas I, Cutts RJ, Pearson A, Tarazona N, et al. Analysis of ESR1 mutation in circulating tumor DNA demonstrates evolution during therapy for metastatic breast cancer. *Science translational medicine.* 2015; 7:313ra182.
49. Segal CV, Dowsett M. Estrogen receptor mutations in breast cancer--new focus on an old target. *Clinical cancer research : an official journal of the American Association for Cancer Research.* 2014; 20:1724–1726. [PubMed: 24583794]
50. Skehan P, Storeng R, Scudiero D, Monks A, McMahon J, Vistica D, et al. New colorimetric cytotoxicity assay for anticancer-drug screening. *Journal of the National Cancer Institute.* 1990; 82:1107–1112. [PubMed: 2359136]
51. Skliris GP, Nugent ZJ, Rowan BG, Penner CR, Watson PH, Murphy LC. A phosphorylation code for oestrogen receptor-alpha predicts clinical outcome to endocrine therapy in breast cancer. *Endocrine-related cancer.* 2010; 17:589–597. [PubMed: 20418363]
52. Tharun IM, Nieto L, Haase C, Scheepstra M, Balk M, Mocklinghoff S, et al. Subtype-specific modulation of estrogen receptor-coactivator interaction by phosphorylation. *ACS Chem Biol.* 2015; 10:475–484. [PubMed: 25386784]
53. Theodorou V, Stark R, Menon S, Carroll JS. GATA3 acts upstream of FOXA1 in mediating ESR1 binding by shaping enhancer accessibility. *Genome research.* 2013; 23:12–22. [PubMed: 23172872]
54. Toy W, Shen Y, Won H, Green B, Sakr RA, Will M, et al. ESR1 ligand-binding domain mutations in hormone-resistant breast cancer. *Nat Genet.* 2013
55. Valley CC, Metivier R, Solodin NM, Fowler AM, Mashek MT, Hill L, et al. Differential regulation of estrogen-inducible proteolysis and transcription by the estrogen receptor alpha N terminus. *Molecular and cellular biology.* 2005; 25:5417–5428. [PubMed: 15964799]
56. Wang P, Bahreini A, Gyanchandani R, Lucas PC, Hartmaier RJ, Watters RJ, et al. Sensitive detection of mono- and polyclonal ESR1 mutations in primary tumors, metastatic lesions and cell free DNA of breast cancer patients. *Clinical cancer research : an official journal of the American Association for Cancer Research.* 2015
57. Wang S, Sun H, Ma J, Zang C, Wang C, Wang J, et al. Target analysis by integration of transcriptome and ChIP-seq data with BETA. *Nat Protoc.* 2013; 8:2502–2515. [PubMed: 24263090]
58. Weir HM, Bradbury RH, Lawson M, Rabow AA, Buttar D, Callis RJ, et al. AZD9496: An Oral Estrogen Receptor Inhibitor That Blocks the Growth of ER-Positive and ESR1-Mutant Breast Tumors in Preclinical Models. *Cancer Res.* 2016

59. Weis KE, Ekena K, Thomas JA, Lazennec G, Katzenellenbogen BS. Constitutively active human estrogen receptors containing amino acid substitutions for tyrosine 537 in the receptor protein. *Mol Endocrinol.* 1996; 10:1388–1398. [PubMed: 8923465]
60. White R, Sjoberg M, Kalkhoven E, Parker MG. Ligand-independent activation of the oestrogen receptor by mutation of a conserved tyrosine. *EMBO J.* 1997; 16:1427–1435. [PubMed: 9135157]
61. Wittmann BM, Sherk A, McDonnell DP. Definition of functionally important mechanistic differences among selective estrogen receptor down-regulators. *Cancer Res.* 2007; 67:9549–9560. [PubMed: 17909066]
62. Yudt MR, Vorojeikina D, Zhong L, Skafar DF, Sasson S, Gasiewicz TA, et al. Function of estrogen receptor tyrosine 537 in hormone binding, DNA binding, and transactivation. *Biochemistry.* 1999; 38:14146–14156. [PubMed: 10571988]
63. Zhang QX, Borg A, Wolf DM, Oesterreich S, Fuqua SA. An estrogen receptor mutant with strong hormone-independent activity from a metastatic breast cancer. *Cancer Res.* 1997; 57:1244–1249. [PubMed: 9102207]
64. Zhao C, Koide A, Abrams J, Deighton-Collins S, Martinez A, Schwartz JA, et al. Mutation of Leu-536 in human estrogen receptor-alpha alters the coupling between ligand binding, transcription activation, and receptor conformation. *The Journal of biological chemistry.* 2003; 278:27278–27286. [PubMed: 12736255]

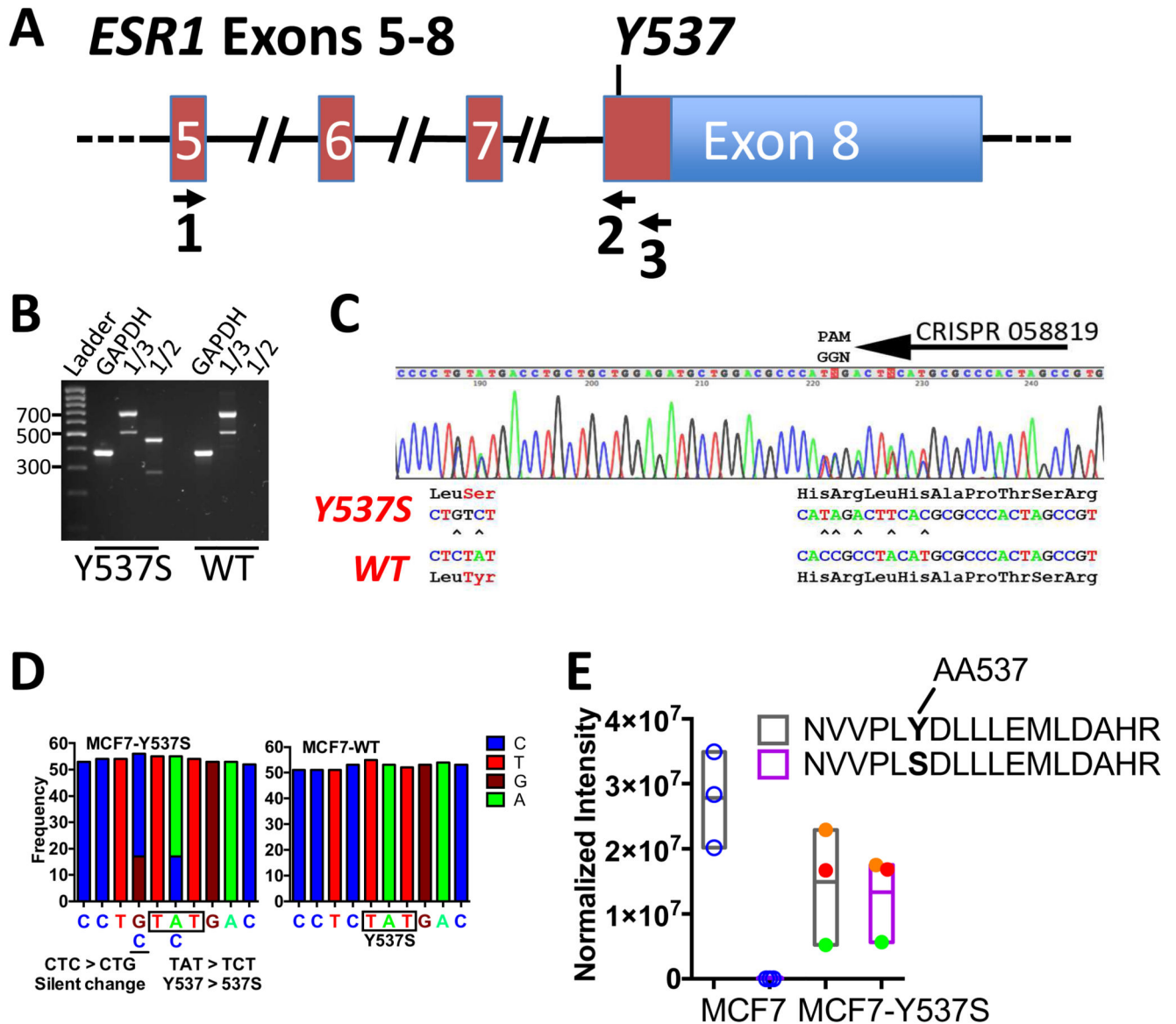


Figure 1. CRISPR-Cas9 directed generation of the Y537S mutation in the *ESR1* gene in MCF7 breast cancer cells.

(A) Schematic representation of the *ESR1* gene, exons 5-8, annotated for the positions of PCR primers used for RT-PCR analysis. (B) RT-PCR of MCF7 (WT) and MCF7-Y537S cell lines using primers in A. Expression of wild-type and mutant ER alleles was confirmed by RT-PCR, using primers in *ESR1* Exon 5 (Primer 1, 5'-CCAGGAAGCTACTGTTTGC-3') and Exon 8 (Primer 3, 5'-GATGCATGCCGGAGTGTATG-3'), which generate a 700bp product. The *ESR1* transcript arising from the Y537S mutant allele was amplified as a 466bp product using the exon 5 primer and the knockin specific primer. (Primer 2, 5'-GATGCATGCCGGAGTGTATG-3'). (C) Sequencing chromatogram of the RT-PCR products for the exon 8 coding region for MCF7-Y537S cells, showing expression of both mutant and wild-type alleles. (D) Frequency of RNA-seq reads for the Y537 and 537S codons in MCF7 and MCF7-Y537S cells. (E) Normalized intensity of ER tryptic peptide

containing amino acid 537 from LC-MS. Results are shown for three independent immunoprecipitated ER samples for MCF7 and MCF7-Y537S lines. No signal was obtained for the mutant peptide in MCF7 cells. For the MCF7-Y537S samples, the normalised intensity for each replicate sample is shown by circles of the same colour, demonstrating similar amounts of the two peptides in MCF7-Y537S cells.

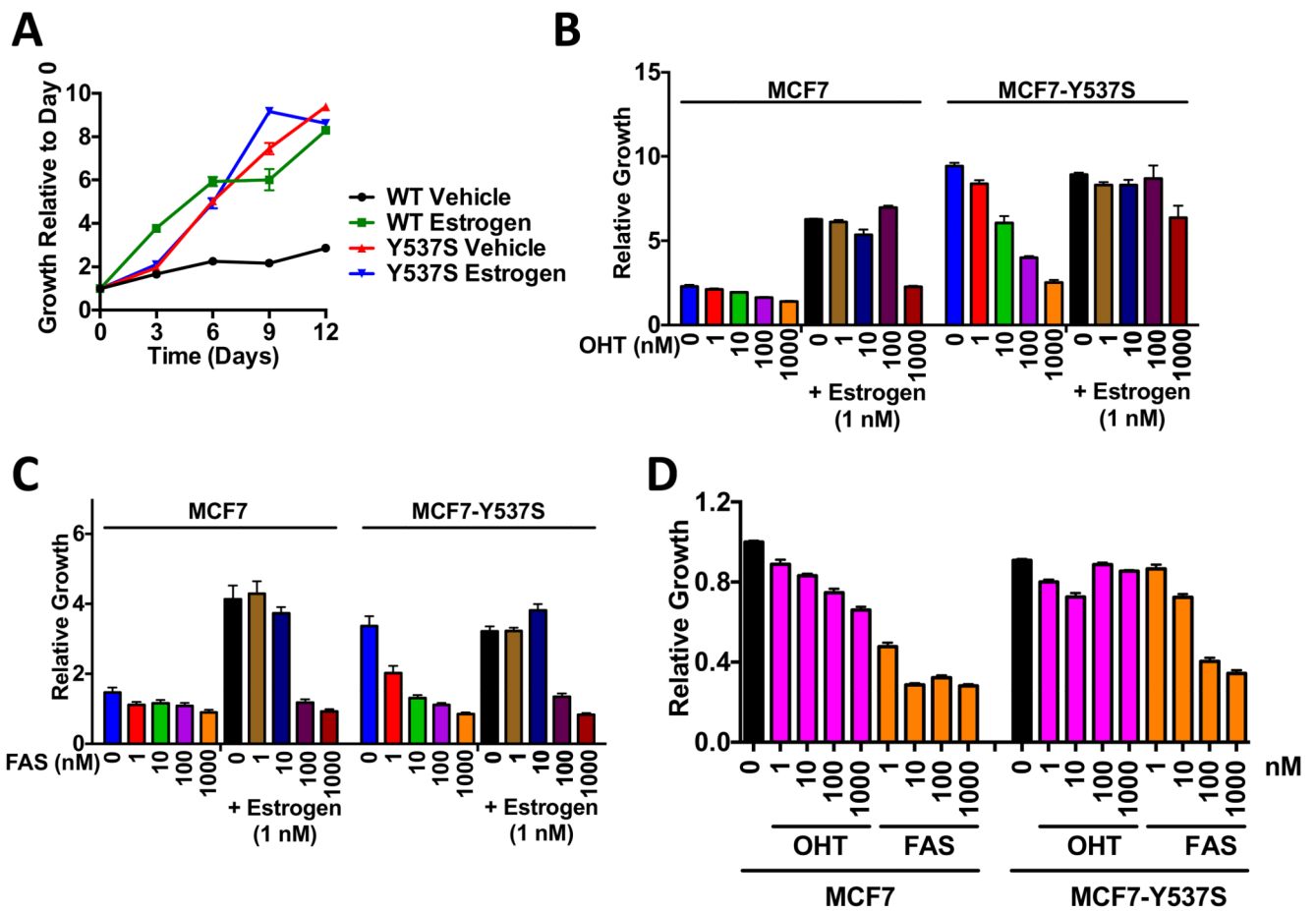


Figure 2. MCF7-Y537S cells grow in an estrogen-independent manner.

(A) MCF7 (WT) and Y537S cells were grown in the absence or presence of 10 nM estrogen over 12 days. (B, C) The cells were grown in the absence of estrogen (vehicle) or in the presence of 10 nM estrogen, together with 0, 1, 10, 100 or 1000 nM 4-hydroxytamoxifen (OHT; B) or flaslodex (FAS; C). Mean growth at day 12 \pm SEM is shown relative to day 0 (n=6). (D) MCF7 and MCF7-Y537S cells, cultured in DMEM+10%FCS, were treated with OHT or FAS at the concentrations shown (nM). The graph shows mean growth at day 12 \pm SEM (n=6).

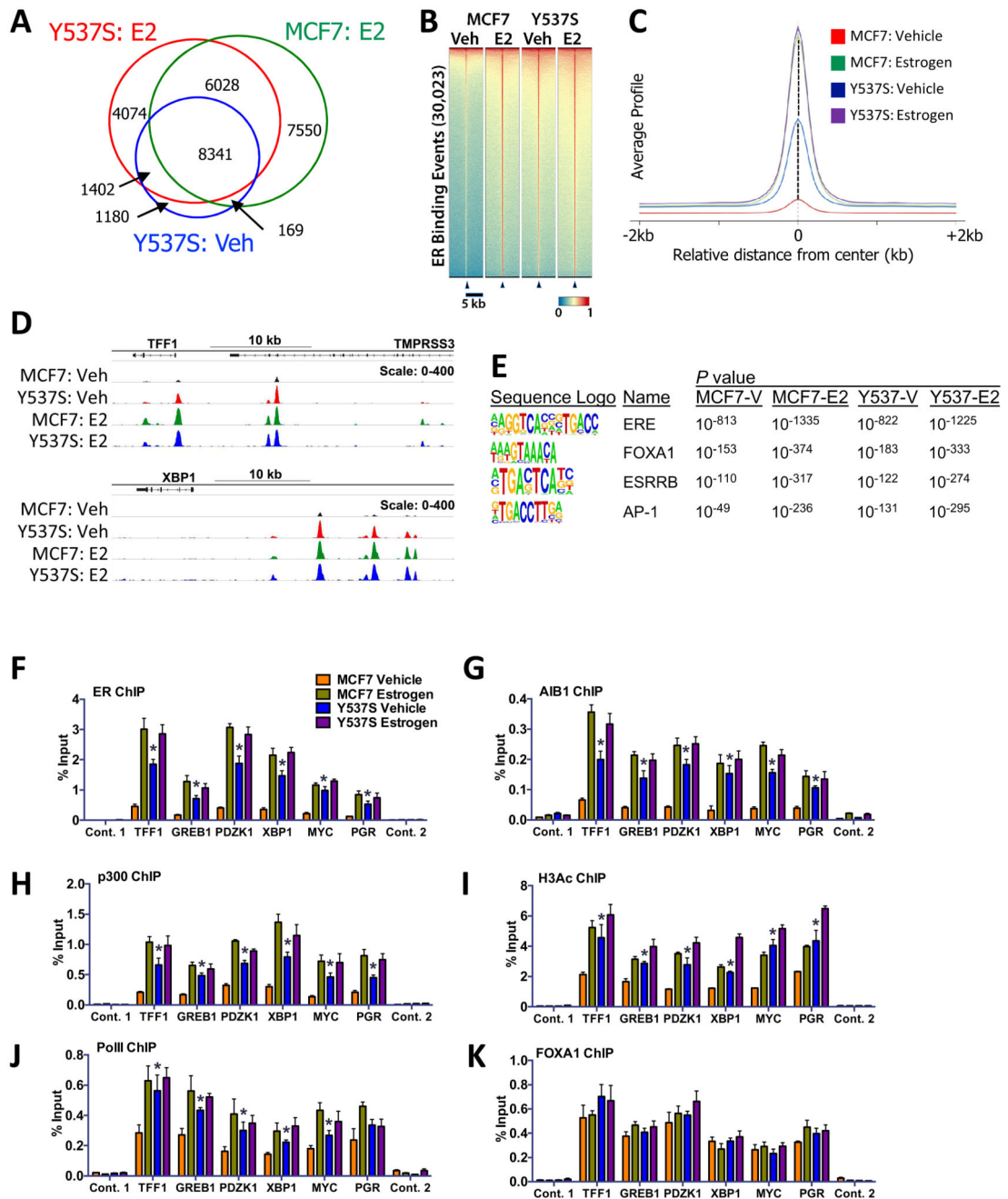


Figure 3. ER-Y537S mutant is globally recruited to ER binding regions in the absence of estrogen.

(A) Overlap of significant ER binding sites as called by MACS analysis ($p < 1 \times 10^{-5}$). (B) Heat map for ER binding events in MCF7 and MCF7-Y537S cells under vehicle (Veh) and estrogen (E2) treatment conditions. (C) Genome-wide profile of ER binding. (D) ChIP-seq tracks showing ER binding at two ER target genes. (E) Shown are the top enriched transcription factor binding motifs obtained using HOMER17. See Supplementary information for a complete list of motifs enriched in MCF7-WT and mutant cells. (F-K) ChIP was performed following treatment of MCF7 and Y537S cells cultured in hormone-

depleted medium and treated with 10 nM estrogen for 45 minutes. Real-time PCR was used to determine enrichment at ER binding regions. PCR for two control regions near the TFF1 (control 1) and the PGR gene (control 2) is also shown. Bar charts represent the mean, \pm SEM (n=3). Asterisks represent statistically significant differences (unpaired t-test, $p < 0.05$) for vehicle-treated MCF7-Y537S cells compared with MCF7 cells.

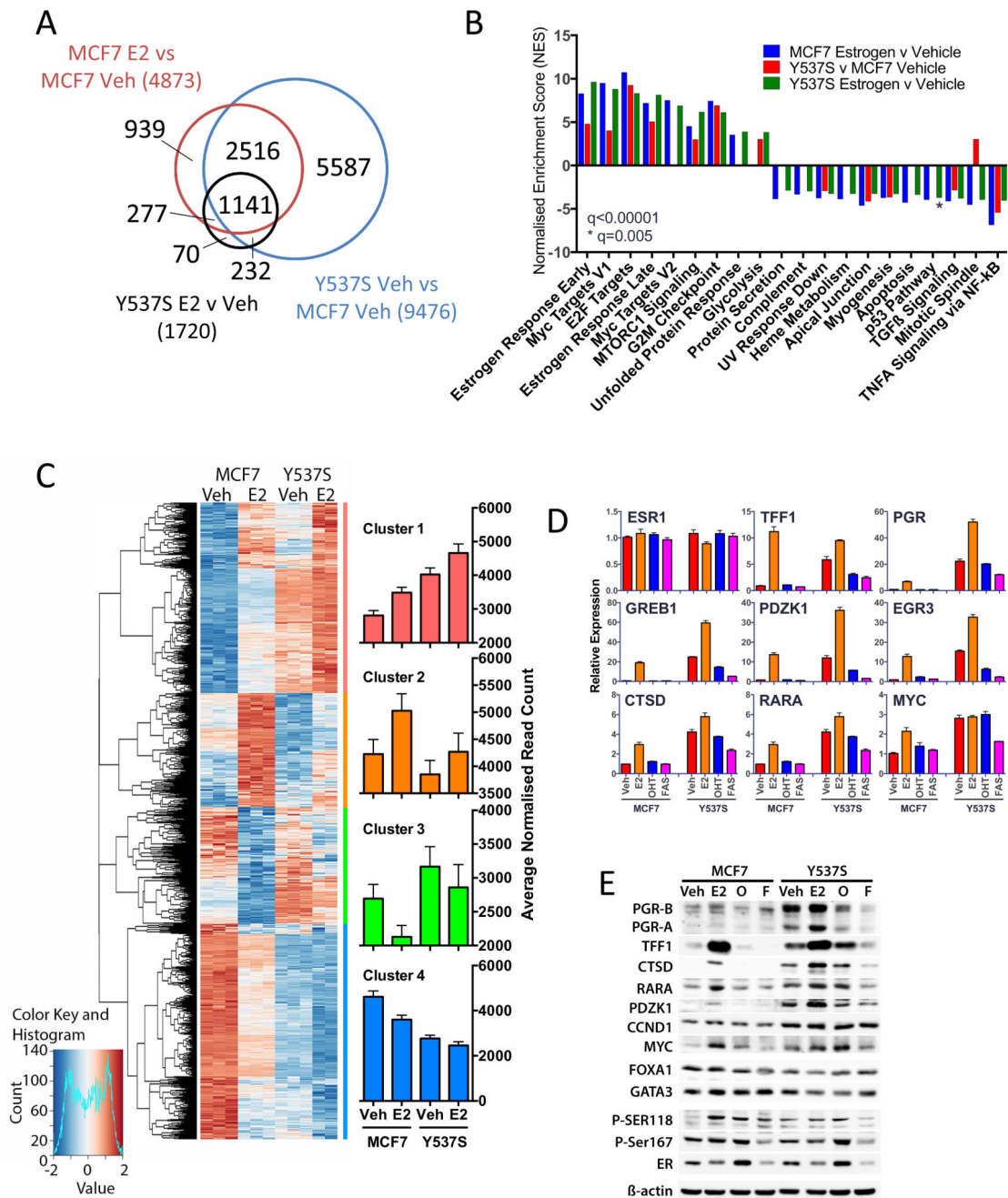


Figure 4. The Y537S mutation promotes estrogen-independent expression of ER target genes in breast cancer cells.

(A) RNA-seq was performed using three replicate samples of hormone-depleted MCF7 and MCF7-Y537S cells, following addition of vehicle or estrogen for 8 hours. Shown is a Venn diagram comparing differentially regulated genes ($\text{padj} < 0.05$) identified from RNA-seq data. (B) The bar chart shows the normalised enrichment scores (NES) from Gene set enrichment analysis (GSEA) for “Hallmark” signaling pathways that are significantly up- or down-regulated ($q < 0.00001$) in pair-wise comparisons of the differentially regulated gene sets. (C) Hierarchical cluster analysis of genes that are differentially regulated in MCF7 cells \pm E2

($p_{adj} < 0.05$) and for which an ER binding site is observed within 100kb of the transcription start site. Barcharts show average normalised counts for all genes in the clusters. (D) E2 (1 nM), OHT (10 nM) or FAS (10 nM) were added to hormone-depleted MCF7 and MCF7-Y537S cells. Shown is RT-qPCR analysis of gene expression using RNA prepared 16 hours following addition of ligands, relative to the vehicle treated MCF7 cells ($n=3$). (E) Immunoblotting was performed using cell lysates prepared 24 hours following addition of ligands.

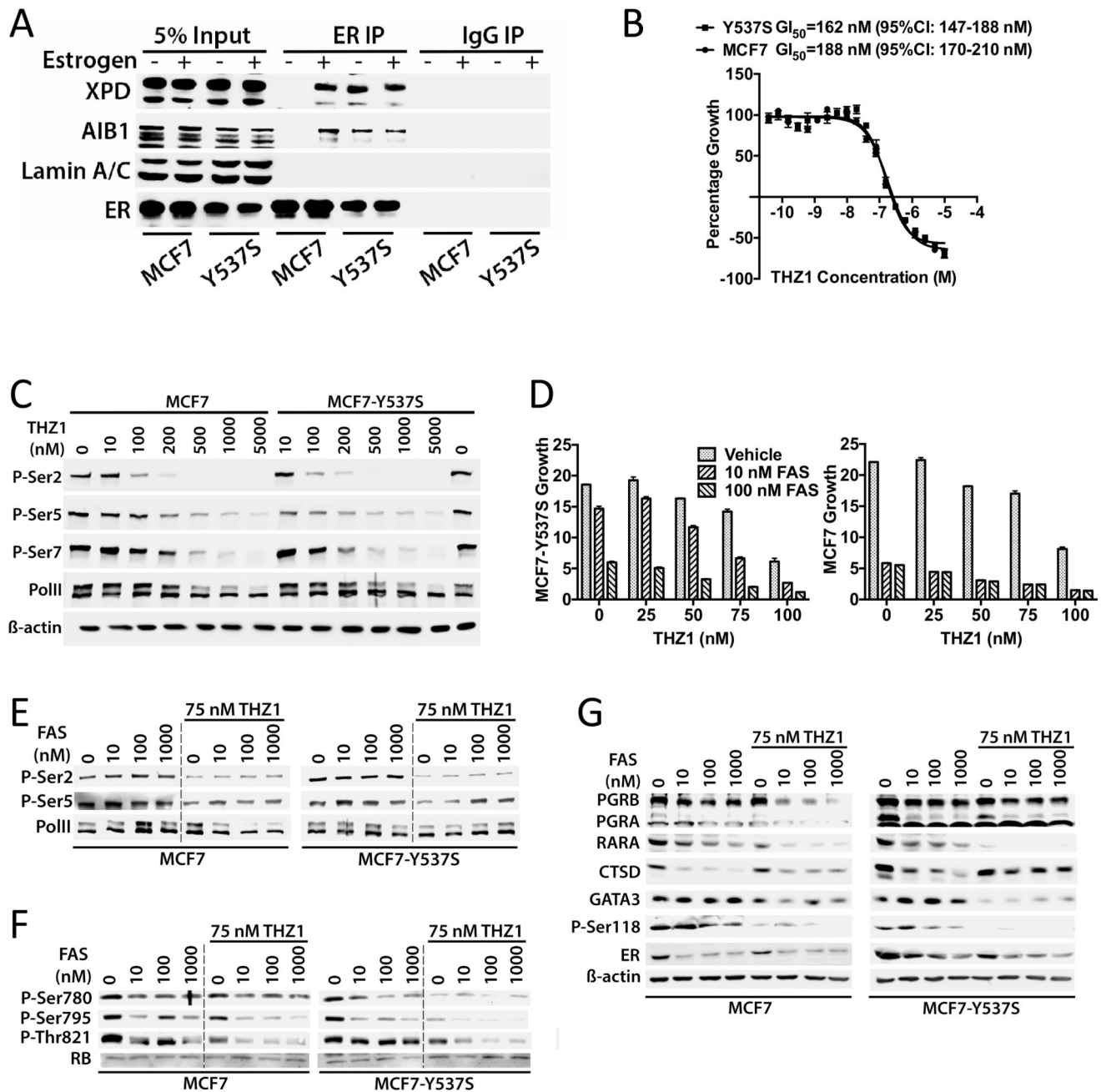


Figure 5. Inhibition of MCF7-Y537S growth by the CDK7 inhibitor THZ1 in combination with anti-estrogens.

(A) TFIIH interacts in an estrogen-independent manner with ER in MCF7-Y537S cells. Protein lysates from hormone-depleted MCF7 and MCF7-Y537S cells treated with estrogen (10 nM) for 3 hours were immunoprecipitated with an antibody for ER, or with mouse immunoglobulins (IgG; control). Immunoprecipitates were immunoblotted with antibodies for the XPD subunit of TFIIH, the ER co-activator AIB1 and a control protein (Lamin A/C). (B) Cells were treated with increasing concentrations of THZ1 for 48 hours. Mean growth is shown relative to that for vehicle (DMSO treated cells) (n=6). GI_{50} = concentration of THZ1

at which cell growth is inhibited by 50%. (C) Protein lysates prepared from cells treated with increasing concentrations of THZ1 for 4 hours, were immunoblotted for PolII and for phosphorylation of Ser2, Ser5 and Ser7 in the PolII C-terminal domain heptapeptide repeat. (D) Cells were grown in DMEM containing 10% FCS over a 12 day period in the presence of 10 or 100 nM FAS, together with 20, 50, 75 or 100 nM THZ1. Growth was assessed using the SRB assay and is shown relative to SRB values at day 0. The bars represent mean values \pm SEM for 6 replicates. (E-G) Immunoblotting was performed with protein lysates prepared 24 hours after addition of FAS \pm 75 nM THZ1.